Metabolic Engineering 69 (2022) 40–49

Contents lists available at ScienceDirect

Metabolic Engineering

journal homepage: www.elsevier.com/locate/meteng

Top-down synthetic biology approach for titer improvement of clinically important antibiotic daptomycin in *Streptomyces roseosporus*

Chang-Hun Ji [a], Hiyoung Kim [a], Hyun-Woo Je [a], Haeun Kwon [b], Dongho Lee [b], Hahk-Soo Kang [a,*]

[a] Department of Biomedical Science and Engineering, Konkuk University, Seoul, 05029, Republic of Korea
[b] Department of Plant Biotechnology, College of Life Sciences and Biotechnology, Korea University, Seoul, 02841, Republic of Korea

ARTICLE INFO

Keywords:
Synthetic biology
Secondary metabolites
Biosynthetic gene clusters
Daptomycin
Production titer

ABSTRACT

Secondary metabolites are produced at low titers by native producers due to tight regulations of their productions in response to environmental conditions. Synthetic biology provides a rational engineering principle for transcriptional optimization of secondary metabolite BGCs (biosynthetic gene clusters). Here, we demonstrate the use of synthetic biology principles for the development of a high-titer strain of the clinically important antibiotic daptomycin. Due to the presence of large NRPS (non-ribosomal peptide synthetase) genes with multiple direct repeats, we employed a top-down approach that allows transcriptional optimization of genes in daptomycin BGC with the minimum inputs of synthetic DNAs. The repeat-free daptomycin BGC was created through partial codon-reprogramming of a NRPS gene and cloned into a shuttle BAC vector, allowing BGC refactoring in a host with a powerful recombination system. Then, transcriptions of functionally divided operons were sequentially optimized through three rounds of DBTL (design-build-test-learn) cycles that resulted in up to ~2300% improvement in total lipopeptide titers compared to the wild-type strain. Upon decanoic acid feeding, daptomycin accounted for ~ 40% of total lipopeptide production. To the best of our knowledge, this is the highest improvement of daptomycin titer ever achieved through genetic engineering of *S. roseosporus*. The top-down engineering approach we describe here could be used as a general strategy for the development of high-titer industrial strains of secondary metabolites produced by BGCs containing genes of large multi-modular NRPS and PKS enzymes.

1. Introduction

Microbial secondary metabolites have traditionally been used as clinically important drugs such as antibacterial, anticancer and immunosuppressive agents to treat life-threatening diseases (Atanasov et al., 2021; Demain, 2014; Patridge et al., 2016). Due to complexities of their chemical structures with many chirality centers, it is often difficult to achieve economically reliable chemical syntheses for secondary metabolite-derived drugs, thus relying their industrial productions on large-scale fermentations of producer microorganisms (Grunewald et al., 2004; Westfall et al., 2012). However, production titers of secondary metabolites from native producers are generally low due to the presence of tight regulatory systems (Lee et al., 2020). The traditional approach of titer improvements has mainly involved repetitive rounds of untargeted, random mutagenesis and subsequent selection of mutants with improved titers (Chen et al., 2009; Gao et al., 2010). Although this approach has resulted in some successful examples, it generally requires a highly labor-intensive and time-consuming selection process as the vast majority of mutations are likely to have negative impacts on metabolite production and/or microbial fitness.

Synthetic biology, represented by the Design-Build-Test-Learn (DBTL) cycle, provides engineering principles that allow the design and build of biological systems with enhanced or new functions (Dahabieh et al., 2020; Palazzotto et al., 2019). There are two main approaches used in synthetic biology. The first one is a “bottom-up approach” in which all required genetic parts are chemically or enzymatically synthesized and assembled into functional biological systems (Smanski et al., 2014). The second one is a “top-down approach” in which existing biological systems are rationally refactored to improve performances or to confer new functionalities (Montiel et al., 2015). These synthetic biology approaches could be applied to engineering secondary metabolite biosynthetic gene clusters (Ajikumar et al., 2010; Song et al., 2019). The biosynthesis of a secondary metabolite drug requires co-expression of biosynthetic, regulatory, and transport genes

* Corresponding author. Department of Biomedical Science and Engineering, Konkuk University, Seoul, Republic of Korea.
E-mail address: hkang@konkuk.ac.kr (H.-S. Kang).

https://doi.org/10.1016/j.ymben.2021.10.013
Received 31 August 2021; Received in revised form 9 October 2021; Accepted 29 October 2021
Available online 2 November 2021

that comprise a biosynthetic gene cluster (BGC) that can span over 50 kb to as large as 200 kb in sizes. Although the use of a bottom-up approach has been reported for small size BGCs, this approach is not a viable option for BGCs containing genes of multi-modular enzymes such as PKSs (polyketide synthases) and NRPSs (non-ribosomal peptide synthetases) due to their large-gene-sizes (>10 kb) with multiple direct repeats, rendering their biological or chemical syntheses technically challenging (Behsaz et al., 2021; Gao et al., 2021). In this case, top-down synthetic biology with the minimum inputs of synthetic DNAs would be a more reliable approach not only to reduce the cost of DNA synthesis but also to minimize unpredictable outcomes of re-designing operon architectures that could make subsequent diagnostic analysis much more complicated (Smanski et al., 2016).

Daptomycin is a clinically important lipopeptide antibiotic, which is considered as an antibiotic of last resort due to its strong activity against methicillin-resistant *Staphylococcus aureus* (MRSA) and distinctive mechanism of action from other antibiotics (Zuttion et al., 2020). Daptomycin is approved for the treatment of complicated skin and soft tissue infections and right-sided infective endocarditis (Gonzalez-Ruiz et al., 2016). Due to its complex chemical structure, daptomycin is industrially produced by the large-scale fermentation of its producer strain *Streptomyces roseosporus*. Unfortunately, daptomycin titers by its wild-type producer are significantly low, as reported titers were 20–40 mg/L in shake-flask cultures (Ye et al., 2014) and 100–120 mg/L in batch fermentations (Lu et al., 2011). Accordingly, several engineering efforts have been made to improve daptomycin titers through perturbation of regulatory genes (Mao et al., 2015, 2017), by conferring resistance to toxic precursors (Lee et al., 2016) or by repetitive accumulation of random mutations (Yu et al., 2011). Of these, the highest titer improvement reported was 380%, which was achieved by random mutagenesis followed by shuffling of beneficial mutations (Yu et al., 2014). This suggests that a more systematic and rational approach would be necessary to develop high daptomycin titer strains suitable for industrial-scale production.

Here, we employed a top-down synthetic biology approach for rational engineering of daptomycin BGC (*dpt* cluster) with an aim to create high daptomycin titer strains (Fig. 1). Using transcriptome analysis, we identified that low transcriptions of genes in the *dpt* cluster are likely to be the main cause of low daptomycin titers in the wild-type producer. Then, one of the NRPS gene *dptBC* was partially codon-reprogrammed to eliminate large direct repeats, and the repeat-free *dpt* cluster was cloned into a shuttle BAC vector to allow BGC refactoring in yeast possessing a powerful recombination system. Next, operon re-structuring and promoter engineering were conducted in a step-wise manner to optimize the transcriptions of genes in the *dpt* cluster, which resulted in up to ~2300% improvement in total lipopeptide titers. Upon decanoic acid feeding, daptomycin production accounted for ~40% of total lipopeptide titers. *S. roseosporus* was further engineered by the deletion of two *bkd* operons involved in biosynthesis of branched chain fatty acids that abolished production of naturally occurring lipopeptides A21978C$_{1\text{-}3}$, and only produced lipopeptides with straight chain fatty acids. The work we describe here highlights the usefulness of top-down synthetic biology for the development of high-titer industrial strains of commercially valuable secondary metabolites.

2. Results and discussions

2.1. Transcriptome analysis of S. roseosporus NRRL 11379

Our initial analysis of the total lipopeptide titer from the native producer *S. roseosporus* NRRL 11379 was approximately 20 mg/L in 50 mL shake-flask cultures. Although the low transcriptional efficiency of genes in the *dpt* cluster has been previously suggested to be the potential main cause of low daptomycin titers, no quantitative analysis has been conducted (Huang et al., 2017; Luo et al., 2018). Thus, we performed a genome-wide transcriptome analysis of *S. roseosporus* at both exponential (3 days) and stationary (5 days) growth phases (Fig. 2; Fig. S1). We inserted the indigoidine synthetase gene (*indC*) under the well-known

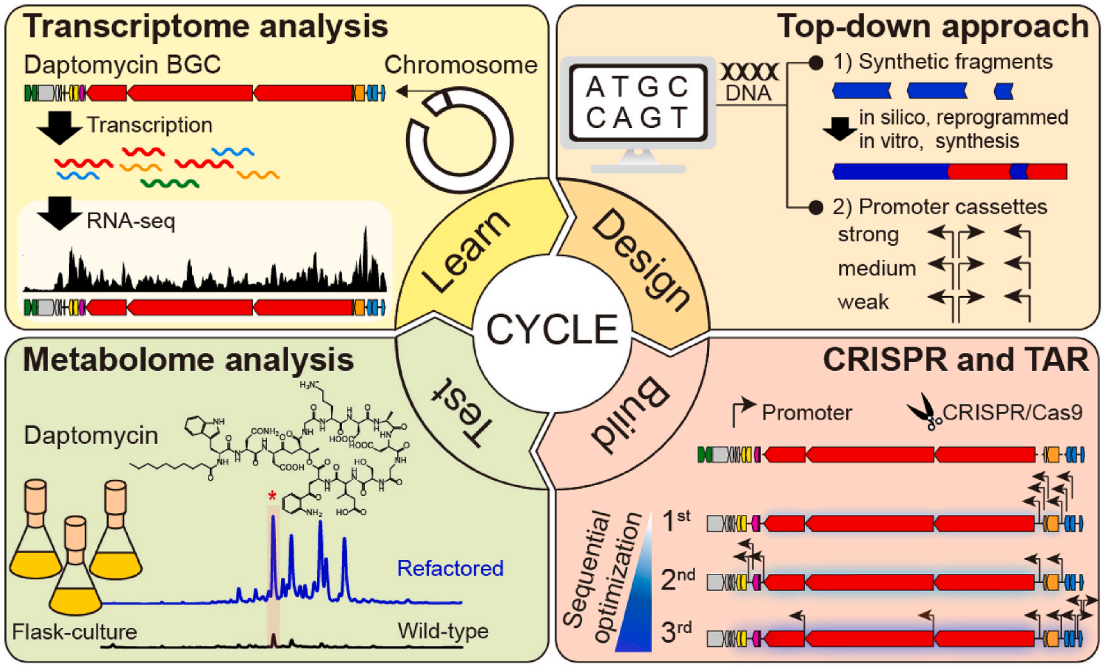

Fig. 1. Schematic illustration of a top-down synthetic biology approach for titer improvement of daptomycin. A design step involves codon-reprogramming, operon re-structuring and designing promoter sequences that are utilized for partial re-factoring of daptomycin BGC. A build step involves the replacement of genetic parts with newly designed sequences using our previously developed CRISTAR (CRISPR/Cas9-mediated TAR) refactoring tool. A test step aims at analyzing the production titer of daptomycin and related lipopeptides for an array of differentially engineered constructs. Lastly, a learn step uses comparative RNA-seq analysis as a tool to identify the potential site of engineering in the next round of engineering. This DBTL (design-build-test-learn) cycle could be repeated several times until we achieve the best production titer.

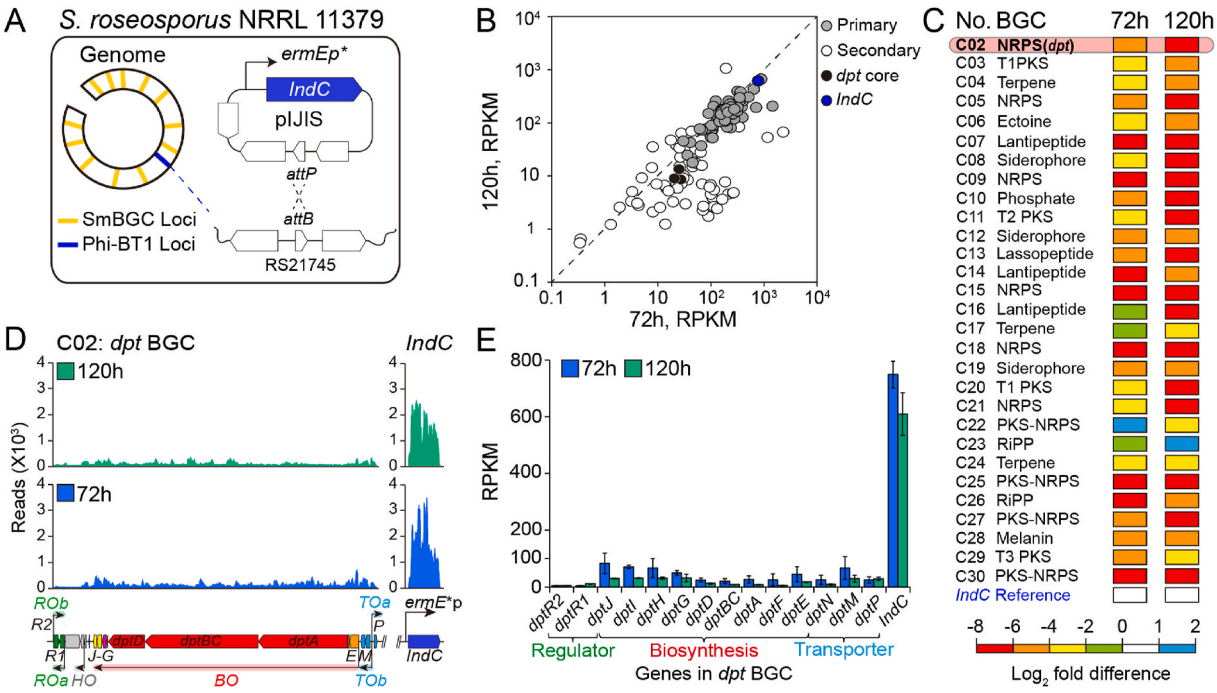

Fig. 2. Genome-wide transcriptome analysis of the native daptomycin producer *S. roseosporus* NRRL 11379. (A) *IndC* (indigoidine synthetase) gene under *ermE**p was integrated into the Phi-BT1 attB site and used as a reference for transcriptome analysis. (B) Scatter plot displaying RPKM values of genes associated with primary metabolisms (gray) and secondary metabolisms (white), genes of *dpt* NRPSs (black) and reference gene (blue) at exponential (72h) and stationary (120h) growth phases. (C) Transcription levels of secondary metabolite BGCs relative to the reference *indC* gene at exponential (72h) and stationary (120h) growth phases. (D) The results of RNA-seq read mapping to the *dpt* cluster and the reference *indC* gene were visualized in the IGB software. Native promoter sites were marked with black arrows. (E) RPKM values of genes in the *dpt* cluster and the reference *indC* gene. Error bars represent standard deviations for duplicate experiments.

Streptomyces constitutive promoter *ermE**p into the *S. roseosporus* genome (Fig. 2A) and used its transcription level as a reference, which displayed the RPKM values of 749 and 609 at exponential and stationary growth phases, respectively (Fig. 2B). *S. roseosporus* harbors the total of 31 secondary metabolite BGCs as determined by antiSMASH (Blin et al., 2019). Of these, two BGCs located at either end (C01 and C31) were excluded from the analysis due to the presence of ambiguous N bases in the sequences. The RNA-seq analysis revealed that transcription levels of genes associated with secondary metabolisms are generally lower compared to genes of primary metabolisms (Fig. 2B). Genes involved in primary metabolisms were transcribed in 10–100% levels of the reference gene. The highest transcription was observed for the gene of GADPH (glyceraldehyde 3-phosphate dehydrogenase) in glycolysis pathway, and their RPKM values (774 in exponential phase and 609 in stationary phase) were nearly identical to those of the reference gene (749 and 609, respectively) in both growth phases. However, transcription levels of genes in secondary metabolisms were significantly lower being mostly less than 30% of the reference gene except for genes from three BGCs including the clusters 17 (terpene), 22 (PKS-NRPS hybrid) and 23 (Ripp) that transcribed strongly during the exponential growth phase (Fig. 2C). In case of the *dpt* cluster, the NRPS genes *dptA*, *dptBC* and *dptD* were among the weakest transcribed genes as their transcription levels were only 1–4% (RPKM values of 5–35) of the reference in both growth phases.

To gain insights into the transcriptional landscape of the *dpt* cluster, we next performed the cluster-level analysis of transcriptome data (Fig. 2D). Transcriptional start sites (TSSs) in the *dpt* cluster were mapped on the basis of differential RNA-seq (dRNA-seq) analysis (Sharma et al., 2010). The total of six primary TSSs were identified, which decompose the *dpt* cluster into six separate operons (Fig. S2). The convergent two single gene operons *ROa* and *ROb* contain genes of pathway-specific regulatory proteins. All genes required for lipopeptide biosynthesis including genes for lipidation (*dptE–F*), peptide extension (*dptA–D*), and precursor biosynthesis (*dptI–J*) are arranged into one large biosynthetic operon (*BO*) transcribed by the promoter located upstream of *dptE* (Fig. S3) (Gal et al., 2006). The divergent operons *TOa* and *TOb* contain genes of three transport proteins, and the last operon *HO* contains a gene of putative phosphatase that has not been characterized to be involved in daptomycin biosynthesis (Miao et al., 2005). The RNA-seq analysis revealed that transcription levels are significantly low in all operons with the RPKM values being only 1–9% of the reference *indC* gene (Fig. 2E). In the previous study, BGCs with RPKM values under 27 were suggested to be silent with their metabolites produced below the detection limit by HPLC (Amos et al., 2017). The RPKM values of three NRPS genes (*dptA*, *dptBC* and *dptD*) in the *dpt* cluster are in the range of 20–30 being close to the detection limit, and thus the low transcriptions of genes in the *dpt* cluster are likely to be one of the major contributing factors to low daptomycin titers in the wild-type producer *S. roseosporus*. Overall, our transcriptome analysis suggests that the transcriptional optimization through BGC refactoring would be a rational approach that can lead to the development of high daptomycin titer strains.

2.2. Cloning of repeat-free daptomycin BGC

BGC refactoring in *Streptomyces* is time-consuming due to the inherent low recombination efficiency. To allow BGC refactoring in a host with a more powerful recombination machinery, we decided to clone the *dpt* cluster, which is approximately 70 kb in size, into a shuttle BAC vector that could replicate in *E. coli*, *Streptomyces,* and yeast (Yamanaka et al., 2014). To this end, we first constructed a fosmid library using the genomic DNA of *S. roseosporus* NRRL11379. Library screening using three primer sets that amplify distal regions in the *dpt* cluster resulted in the recovery of three overlapping fosmids. Recovery of the complete *dpt* cluster was confirmed by end-sequencing of each fosmid (Fig. S4). The overlapping fosmids were assembled, and the complete *dpt* cluster was captured into a shuttle BAC vector using TAR (Transformation-Associated Recombination) in yeast (Kim et al., 2010),

creating the construct BAC-*dpt*. Although the successful cloning was confirmed by PCR-based genotyping, the cloned *dpt* cluster was highly unstable in yeast and in *E. coli* as we frequently observed the BAC-*dpt* DNA splitting into multiple bands over time in agarose gel electrophoresis (Fig. S5). To find the possible cause of this, we analyzed the DNA sequence of the *dpt* cluster and identified the presence of a number of large direct repeats (>100 bp) within the second NRPS gene *dptBC* (Table S4). The presence of large direct repeats is a common phenomenon for genes encoding multi-modular enzymes such as PKSs and NRPSs because domain duplications have been known to be one of the main drivers of genetic diversifications (Gotze et al., 2019; Song et al., 2020). Since the presence of large direct repeats could cause unexpected cross-recombination between repeat sequences during recombination-based BGC refactoring in yeast resulting in partial truncations of the cluster (Sharan et al., 2009), we sought to eliminate all direct repeats that are larger than 100 bp in sizes.

Our analysis indicated that the *dptBC* gene contains the total of 28 direct repeats with the sizes larger than 100 bp (Fig. 3A). The largest direct repeat was 1271 bp that lies in epimerase domains between the modules 8 and 11 (repeat 1). For most of the direct repeats, one sequence lies in the first half of *dptBC* between the modules 6 and 8 (segment A), and the other sequence in the second half between the modules 9 and 11 (segment B). Thus, these direct repeats could be eliminated by codon-reprogramming of the segment B region. There was one sequence that repeats three times (repeat 5), one in the segment B and two in the segment A, that could be eliminated by codon-reprogramming of the small part (part A) in the segment A region. To this end, new codon-reprogrammed sequences were designed for the segment B and part A regions by replacing existing codons with synonymous codons. Overall codon usage frequencies were kept constant to avoid any potential translational bottleneck. The *in-silico* analysis confirmed that the re-designed *dptBC* gene sequence (*dptBC**) is free of large direct repeats while translating into the same amino acid sequence. Therefore, the DNA sequences of segment B (~10 kb) and part A (~2 kb) were chemically synthesized, and the synthetic DNAs were incorporated into the *dptBC* gene using CRISTAR (CRISPR/Cas9-mediated TAR) in yeast (Kim et al., 2020). The complete *dptBC** gene (22 kb) was cloned into a BAC vector, creating the construct BAC-*dpt/Middle*. The downstream (26 kb) and upstream (32 kb) regions of *dptBC* were also separately cloned into the same BAC vector yielding the constructs BAC-*dpt/Front* and BAC-*dpt/Back*, respectively (Fig. S6). The three separate constructs were assembled into the complete *dpt** cluster and captured into the BAC vector, creating the final construct of BAC-*dpt** (Fig. 3B). The successful cloning of the complete *dpt** cluster was confirmed by PCR-based genotyping and NGS sequencing on the Illumina platform. The cloned *dpt** cluster was stable in yeast and *E. coli* over a long period of time, as no splitting of the DNA band was observed in the repetitive analysis by gel electrophoresis (Fig. S7).

2.3. Lipopeptide productions in heterologous and native hosts

With the repeat-free *dpt** cluster cloned in the BAC vector, we next compared lipopeptide titers in both heterologous and native hosts to determine the best suitable host for lipopeptide production. The BAC-*dpt** construct was conjugated into the three well-known heterologous hosts *S. lividans*, *S. coelicolor* and *S. albidoflavus* J1074 using intergenic

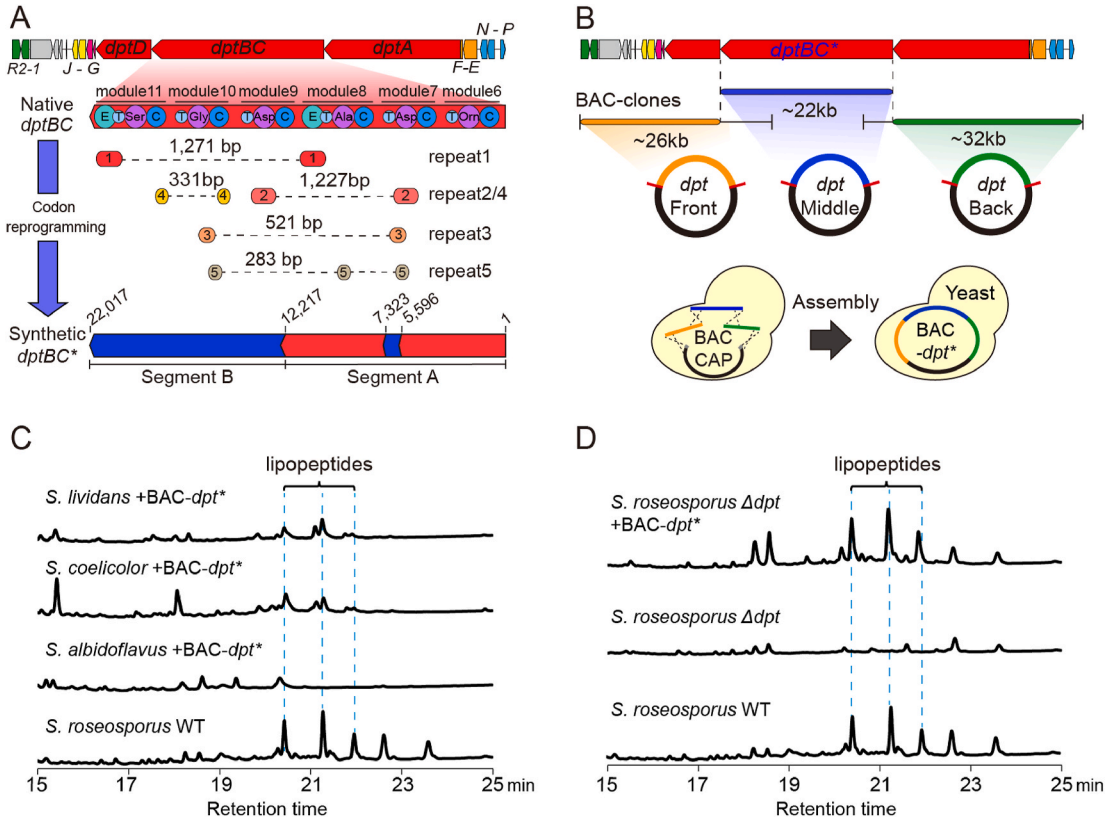

Fig. 3. Cloning of the repeat-free *dpt* cluster, and its expression in heterologous and native hosts. (A) Partial codon-reprogramming of *dptBC* for the removal of large direct repeats. Direct repeats with sizes larger than 250 bp were shown. The codon-reprogrammed regions (highlighted in blue) in *dptBC** were chemically synthesized to create the partially synthetic *dptBC** gene. (B) TAR assembly of three *dpt* fragments. BAC-*dpt*/Front represents the region upstream of *dptBC**. BAC-*dpt*/Middle contains the codon-reprogrammed *dptBC** gene. BAC-*dpt*/Back includes the region downstream of *dptBC**. All three fragments contain 500 bp overlapping sequences to facilitate the DNA assembly. (C) HPLC analyses of three *Streptomyces* heterologous hosts harboring the *dpt** cluster. (D) HPLC analyses of wild-type strain, *dpt* cluster deletion strain and the *dpt* cluster deletion strain complemented with the cloned *dpt** cluster. HPLC peaks of naturally occurring lipopeptides A21978$C_{1\text{-}3}$ were highlighted using light-blue dotted lines.

conjugation and integrated into the genomes using ΦC31 integrase. The heterologous hosts harboring BAC-*dpt** were grown in R5A rich media under the identical growth condition, and *dpt*-related lipopeptide productions were quantitatively analyzed by HPLC. Lipopeptide production was observed in *S. lividans* and *S. coelicolor*; however, no production was seen in *S. albidoflavus* J1074 (Fig. 3C). When compared with the native producer *S. roseosporus*, the production levels were significantly lower (10–12 mg/L) in the heterologous hosts. This suggests that *S. roseosporus* would be the most suitable host for lipopeptide production. To take full advantage of *S. roseosporus* as a host for the expression of refactored *dpt** clusters without any regulatory interference, we deleted the entire endogenous *dpt* cluster using CRISPR/Cas9-based genome editing (Cobb et al., 2015). The *dpt* cluster-deletion strain *S. roseosporus* Δ*dpt* completely abolished lipopeptide production, which was recovered upon re-introduction of BAC-*dpt** into the ΦC31 attB site (Fig. 3D). Lipopeptide titers (20–30 mg/L) were also nearly identical between the wild-type strain *S. roseosporus* and the strain *S. roseosporus* Δ*dpt* + BAC-*dpt**.

2.4. Step-wise transcriptional optimization of daptomycin BGC

Since our transcriptome analysis suggested that low transcriptions of genes are likely to be one of the main causes of low lipopeptide titers in the wild-type strain, we next aimed for transcriptional optimization of the *dpt** cluster. Promoter engineering was performed using our previously published mpCRISTAR (multiple plasmid-based CRISPR/Cas9 and TAR) platform (Fig. S8A) (Kim et al., 2020). It has been known that when replacing multiple promoters, the combination of the strongest promoters does not always lead to the best outcome due to the nonlinearity of biological systems (Alper and Avalos, 2018). Thus, we employed a sequential optimization approach in which transcriptions of functionally separated operons were optimized in a stepwise manner. For use in promoter engineering, we first tested the transcriptional strengths of total 24 promoter sequences from our in-house promoter library in *S. roseosporus* using the *indC* gene-based reporter system, which classified promoters into weak, medium, and strong promoters based on the observed OD_{600} values (Fig. 4A; Fig. S8B) (Ji et al., 2018). As determined by dRNA-seq, the *dpt** cluster mainly consists of six operons that could be functionally categorized into four distinct groups. We first deleted the two regulatory operons *ROa* and *ROb* each containing the pathway-specific regulatory genes *dptR1* and *dptR2*, respectively (Fig. S9) (Wang et al., 2014; Yu et al., 2020), and the deletion of regulatory genes had no effect on total lipopeptide titers (Fig. S9C). The large biosynthetic operon (*BO*) contains all genes required for daptomycin biosynthesis (*dptE–J*) with *dptEp* (P1) as a sole promoter driving its transcription, thus generating a remarkably long 52 kb mRNA transcript. However, in our RNA-seq analysis significant attenuation in transcription was observed within the *dptE* gene that could potentially cause low transcriptions of downstream NRPS genes regardless of the promoter strength of *dptEp*. We experimentally verified this possibility using our *indC* gene-based reporter system (Fig. S10). When the *indC* gene was cloned after the *dptE&F* genes, the expression level decreased by approximately 3-fold compared to the *indC* gene cloned right under the promoter *dptEp*. Based on this observation, we added the additional

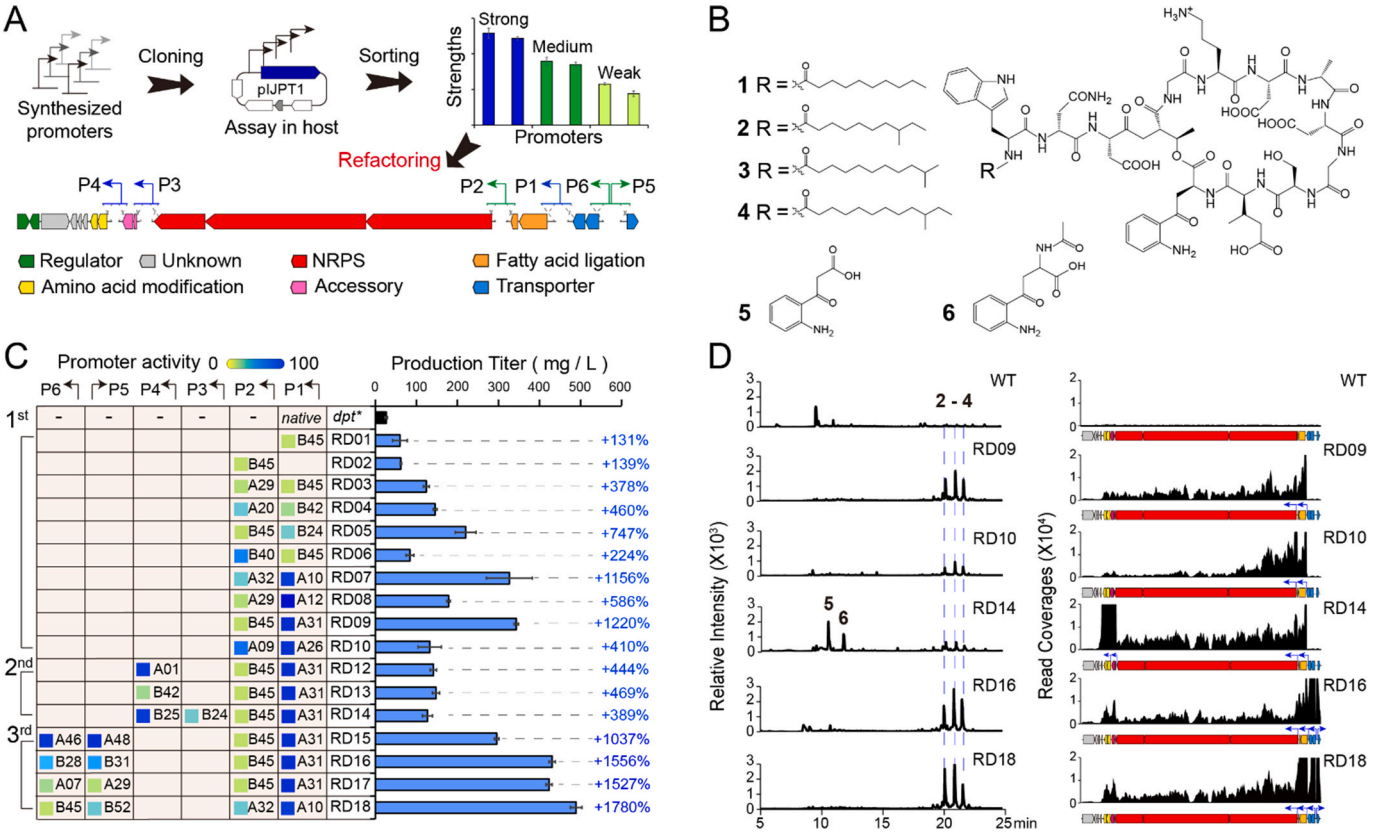

Fig. 4. Promoter engineering of *dpt** cluster. (A) Schematic illustration of our promoter engineering strategy. Diverse promoters different in strengths were used for promoter engineering to generate the library of refactored constructs with different promoter combinations. (B) Structures of daptomycin (**1**), naturally occurring lipopeptides A21978$C_{1\text{-}3}$ (**2**–**4**) and metabolites observed from the promoter-engineered construct RD14 (**5** and **6**). The structures of **5** and **6** were determined as 3-oxo-3-(2-aminophenyl) propionic acid and N-acetyl kynurenine, respectively. (C) Promoter combinations and lipopeptide titers in shake-flask cultures for promoter-engineered *dpt** constructs (RD1-RD18). The best titer was observed from the construct RD18 that showed the lipopeptide production of 489.1 mg/L, 1780% improvement from the wild-type. Error bars represent standard deviations for three biological replicates. (D) HPLC and RNA-seq analyses of *S. roseosporus* harboring the promoter-engineered *dpt** constructs.

promoter site (P2) in front of the first NRPS gene *dptA* (Fig. 4A and Fig. S11).

Then, we performed the first round of promoter engineering on two promoter sites (P1 and P2) as these two promoters drive the transcriptions of all biosynthetic genes, and thus their optimization would most strongly affect lipopeptide titers. The first round of promoter engineering generated the total of 10 different constructs (RD1-10 in Fig. 4C) with diverse combinations of promoters different in transcriptional strengths. Increases in lipopeptide titers were observed from all of the constructs with RD9 representing the highest titer improvement (1220%), which harbors the strong promoter (A31) on P1 and weak promoter (B45) on P2. The RD10 construct containing two strong promoters (A26 & A09) and RD3 containing two weak promoters (B45 & A29) showed less improvements (410% and 378%, respectively) compared to RD9 although no difference in growth rate was observed. The comparison of RNA-seq data between RD10 and RD9 revealed that RD10 has a higher transcription level near the P2 TSS, but the lower level in the distal end probably due to more severe transcriptional attenuation (Fig. 4D).

Since RD9 yielded the best result in the first round, we used this construct for the second round of promoter engineering. Due to transcriptional attenuation, the four genes *dptG-J* located downstream of the NRPS genes display very weak transcriptions, and thus we added the two additional promoter sites P3 and P4 in front of *dptG* and *dptI*, respectively. The genes *dptG* and *dptH* encode MbtH-like protein and alpha/beta hydrolase (type II thioesterase), respectively, thus playing a role as NRPS accessory proteins, whereas the proteins of *dptI* and *dptJ* are responsible for amino acid modification hence precursor biosynthesis (Liao et al., 2013b; Nguyen et al., 2006). Promoters on the P3 and P4 sites drive the transcriptions of NRPS accessory genes and precursor biosynthesis genes, respectively. The three constructs (RD12-14) were generated through the second round of promoter engineering. However, lipopeptide titers decreased in all three constructs by nearly half as compared to RD9. When the strong promoter was inserted on P4 (RD14), we observed a significant decrease in the lipopeptide titer while accumulating new metabolites (**5** and **6**) in HPLC analysis. The structure determination by HRMS and 2D NMR analysis (Figs. S12–S13) indicated that compounds **5** and **6** are 3-oxo-3-(2-aminophenyl) propionic acid and N-acetyl kynurenine, respectively (Fig. 4B). The gene *dptJ* encodes the enzyme tryptophan 1,3-dioxygenase that catalyzes the conversion of tryptophan to N-formyl kynurenine in kynurenine pathway (Zummo et al., 2012). The accumulation of **5** probably indicates that this enzyme is also able to accept indole 3-acetic acid as a minor substrate upon overexpression. The low lipopeptide titer together with the accumulation of **5** and **6** in RD14 indicates that the over-expression of *dptJ* has probably reduced the intracellular concentration of tryptophan, which is also the precursor of *dpt*-related lipopeptides.

As all of the constructs in the second round of promoter engineering showed no titer improvement, we proceeded to the third round with the RD7 and RD9 constructs, which was aimed at engineering the divergently placed P5 and P6 promoter sites that drive the transcriptions of transport operons *TOa* and *TOb*. Through the third round of engineering, we generated the total of four constructs (RD15-18). Of these, the three constructs RD16-18 displayed higher lipopeptide titers compared to RD9, whereas lower titer was observed from RD15, which contain strong promoters on both sites. The highest titer improvement, 50% from RD7 and 1780% (489 mg/L) from wild-type, was observed from RD18 that harbors the medium promoter (B52) on P5 and weak promoter (B45) on P6. This result suggests that the transport proteins encoded by *dptN-P* would play important roles in both importing precursors and exporting lipopeptides (Baltz, 2021; Zhang et al., 2021), thus contributing significantly to lipopeptide titers. Despite the use of low-density flask cultures, the lipopeptide titer observed from the culture of RD18 surpassed titers reported using the wild-type strain cultivated in high-density batch fermentation (Ng et al., 2014).

Although varying in degrees, RNA-seq analyses of engineered constructs all exhibited a gradual decline in transcript abundance in the extremely long biosynthetic operon (approximately 46.6 kb) containing three NRPS genes probably due to the occurrence of prematurely terminated transcripts. This suggests that the insertion of additional promoters in front of *dptBC** (P7) and *dptD* (P8), which are located distant from the TSS, would further increase lipopeptide titers by reducing transcriptional attenuations. Since the coding regions of NRPS genes are overlapped between each other by 4 bp, we physically separated them and inserted weak promoters onto the P7 and P8 sites using RD17 and RD18 as engineering templates, creating the two additional constructs RD19 and RD20, respectively (Fig. 5A). However, no improvement in lipopeptide titers was observed from both constructs compared to RD17 and RD18 (Fig. 5B), although the RNA-seq analysis suggested 40% and 25% increase in transcription levels for *dptBC** and *dptD*, respectively (Fig. 5C). Since no significant growth rate change was observed from RD19 and RD20 compared to the wild-type (Fig. S14), the decreases in lipopeptide titers could be attributed to lower translation rates caused by shorter mRNA transcripts. *Lim* et al. previously demonstrated that the translation initiation rate from an mRNA is 6-fold higher during transcription than after its release, and as a result gene expression could increase by ~ 40% for each 1 kb transcription distance (Lim et al., 2011). It is also probable that 4 bp overlapping sequences between the contiguous NRPS genes (*dptA–BC and dptBC–D)* would be an optimal intergenic distance for re-initiation of translation (Tian and Salis, 2015).

2.5. Daptomycin production upon decanoic acid feeding

All naturally occurring lipopeptides (A21978$C_{1\text{-}3}$, **2**–**4** in Fig. 6B) produced by *S. roseosporus* contain branched medium-chain fatty acids as a lipid moiety, while the commercial antibiotic daptomycin is made of the straight chain decanoic acid (**1** in Fig. 6B). Thus, we next analyzed the production of daptomycin upon decanoic acid feeding in *S. roseosporus* harboring promoter-engineered *dpt** constructs (Fig. 6). Decanoic acid has been known to be toxic at high concentrations (Huber et al., 1988; Liao et al., 2013a), and thus we introduced the additional copy of *dptE&F* genes under the strong promoter *KasOp** (Fig. 6A), as they encode proteins that catalyze the conversion of decanoic acid into less toxic decanoyl-ACP (Wittmann et al., 2008). Then, the strain *S. roseosporus* Δ*dpt* + RD18 with or without the additional copy of *dptE&F* was grown in the presence of decanoic acid at the final concentration of 0.5 mM, and daptomycin production titers were compared (Fig. 6C). The strain with the additional copy of *dptE&F* showed 17% improvement in the total lipopeptide titer (615 mg/L), and daptomycin accounted for 36% (220 mg/L) of the total lipopeptide production.

Since naturally occurring lipopeptides still occupy approximately 64% of the total lipopeptides, we next wanted to see if we can increase the proportion of daptomycin by removing the endogenous biosynthetic pathway of BCFAs (branched chain fatty acids) in *S. roseosporus*. This assumption was based on the comparative analysis of RNA-seq data between the wild-type and lipopeptide-overproduced strains. *S. roseosporus* harbors two copies of the *BKD* (branched chain α-keto acid dehydrogenase enzyme complex) operon comprised of the three genes *bkdA-C* that encode enzymes involved in the early stage of BCFA biosynthesis. Transcriptions of the *BKD* operons were markedly increased (17–22 folds) in *S. roseosporus* harboring the promoter-engineered *dpt** construct (Fig. S15), suggesting that these operons are primarily responsible for maintaining the intracellular level of BCFAs. The approximately 25 kb genomic region that contains the two *BKD* operons was completely deleted using CRISPR/Cas9-based genome editing (Cobb et al., 2015), and the successful deletion was confirmed by PCR-based genotyping and Sanger sequencing (Fig. S16). In the HPLC analysis, the peaks of three naturally occurring lipopeptides (A21978$C_{1\text{-}3}$) disappeared in the *BKD* operon deletion strain and instead, new peaks **7** and **8** appeared although the total lipopeptide titer was significantly lower (198 mg/L) (Fig. 6D; Fig. S17). The LC-MS

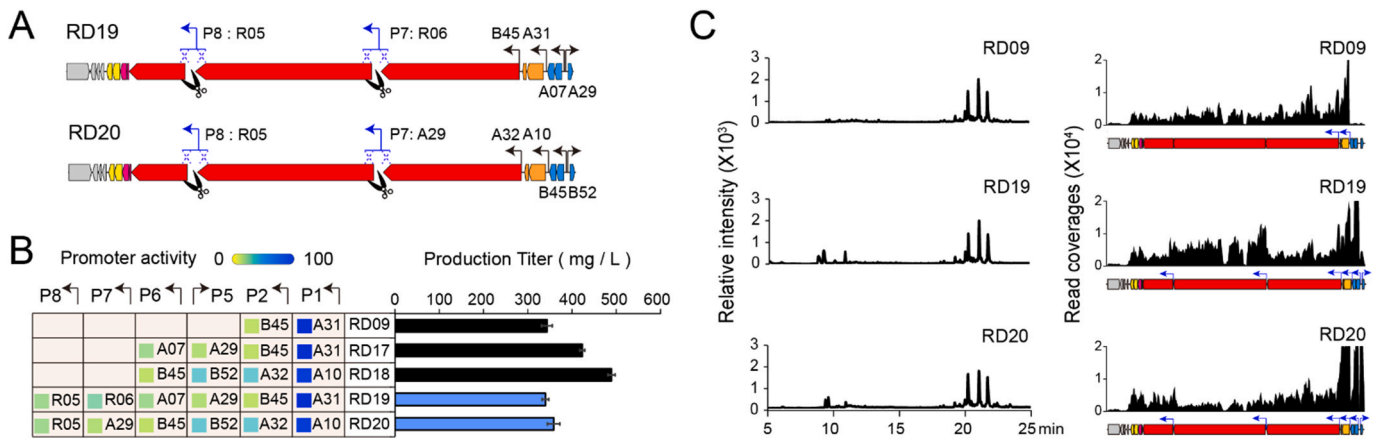

Fig. 5. Promoter insertions in front of *dptBC** and *dptD* and their effects on lipopeptide titers. (A) Illustration of additional promoter engineering strategy. Weak or medium promoters were inserted in front of *dptBC** (P7) and *dptD* (P8) using mpCRISTAR, creating the two additional promoter-engineered *dpt** constructs RD19 and RD20. (B) Promoter combinations and lipopeptide titers in shake-flask cultures for RD19 and RD20. (C) HPLC and RNA-seq analyses of *S. roseosporus* harboring RD19 or RD20 in comparison to RD9.

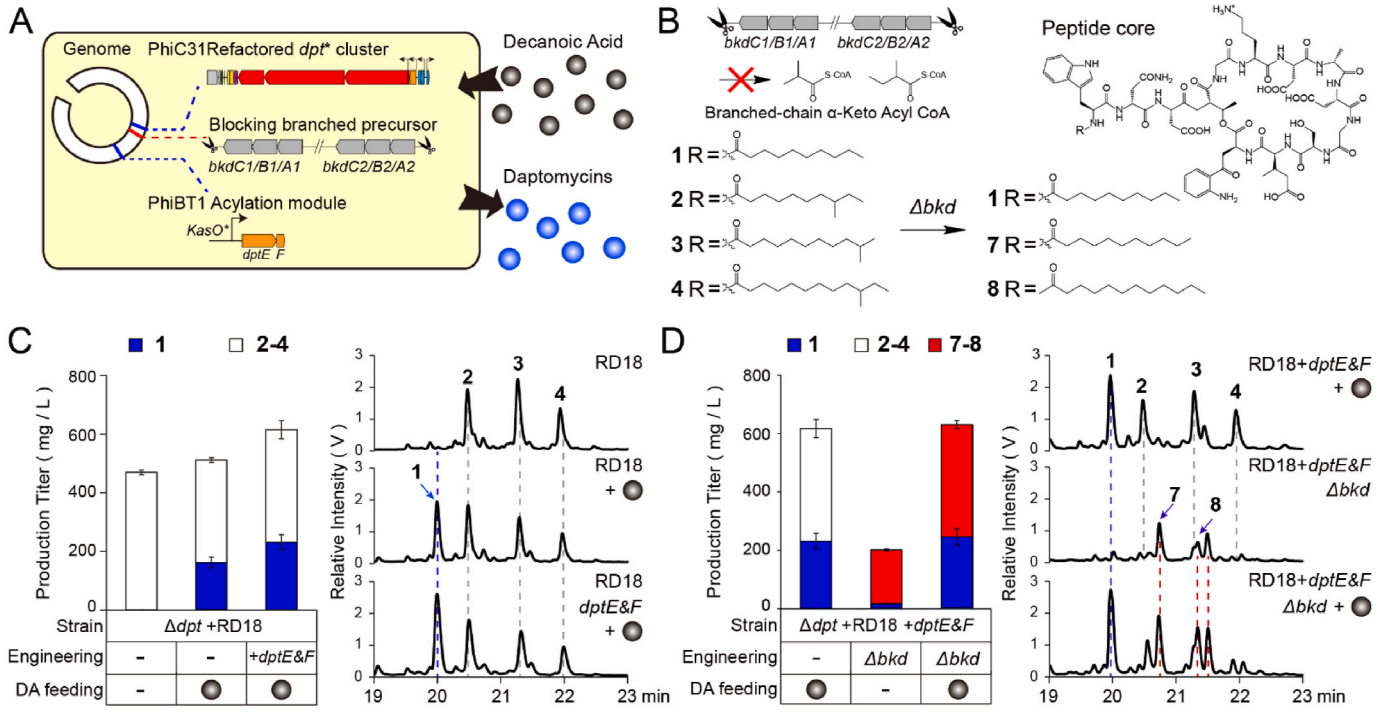

Fig. 6. Production of daptomycin and related lipopeptides upon decanoic acid feeding. (A) Illustration of genome engineering strategy and decanoic acid feeding for daptomycin production. The additional copy of *dptE&F* genes under the strong promoter *kasOp** was introduced into the genome of *S. roseosporus*, while two copies of *bkd operons* were deleted. The effects of genome engineering on lipopeptide titers were evaluated using shake-flask cultures. (B) The structures of daptomycin (**1**), lipopeptides with branched chain fatty acids (**2**–**4**) observed from strains with *bkd* operons and lipopeptides with straight chain fatty acids (**7** and **8**) observed from *bkd* operon deletion strains. (C) The effect of additional *dptE&F* overexpression on the production titers of daptomycin and related lipopeptides upon decanoic acid feeding (DA feeding). (D) The effect of *bkd* operon deletion on the production titers of daptomycin and related lipopeptides upon decanoic acid feeding (DA feeding).

analysis determined the molecular weights of **7** and **8** as 1634 and 1648 (Fig. S18), which correspond to the lipopeptides with C11 and C12 straight chain fatty acids (SCFAs), respectively (Debono et al., 1987). Upon decanoic acid feeding, the total lipopeptide titer was recovered to 627 mg/L, which corresponds to 2312% improvement from the wild-type strain, and daptomycin accounted for 37% (230 mg/L) of the total lipopeptides (Fig. 6D). This result suggests that in the *bkd* operon deletion strain, the intracellular pool of BCFAs was replaced with SCFAs, and the substrate specificities of *dptE&F* towards branched and straight chain FAs are not significantly different, and thus the spectrum of lipopeptide production would depend on the intracellular pool of fatty acids.

3. Conclusions

Production titers of secondary metabolites are generally low in most wild-type producers, which is mainly due to tight transcriptional controls of their BGCs. This hampers the use of wild-type strains for industrial-scale productions of secondary metabolites. Synthetic biology provides engineering principles for rational refactoring of BGCs to achieve transcriptional optimization of genes without regulatory interference. Here, we employed this synthetic biology approach for titer

improvement of clinically important antibiotic daptomycin, which is biosynthesized by a large multi-modular NRPS gene cluster. Genome-wide transcriptome analysis of the wild-type producer *S. roseosporus* demonstrated that low transcriptions of genes in BGC are the major contributor to low daptomycin titers. Then, we eliminated large direct repeats through the partial chemical synthesis of codon-reprogrammed *dptBC** and cloned the repeat-free *dpt** cluster into the shuttle BAC vector, thereby enabling BGC refactoring in a host with a powerful recombination system. For transcriptional optimization, we divided the *dpt** cluster into functionally separate operons that were transcriptionally optimized in a stepwise manner through three DBTL cycles, which resulted in up to ~2300% improvement in total lipopeptide titers compared to the wild-type strain. To the best of our knowledge, this is the highest improvement in lipopeptide titers ever achieved through genetic engineering of *S. roseosporus*. The total lipopeptide titer in the flask culture reached approximately 627 mg/L, and upon decanoic acid feeding, the titer of daptomycin accounted for approximately 37% of the total lipopeptide titer (230 mg/L). We expect that the use of fed-batch fermentation to reach high cell densities and continuous feeding of decanoic acid into fermentation media will bring daptomycin titers easily above the commercial-scale (>1 g/L).

Low transcriptions of genes in BGCs are likely to be a general phenomenon for secondary metabolites with low production titers. Thus, transcriptional optimization of genes would be critical for maximizing production titers especially in hosts with sufficient precursor supplies. Although synthetic biology has provided tools for rational refactoring of BGCs, its application to BGCs containing genes of multi-modular NRPS and type I PKS enzymes has been limited due to their large-sizes (typically over 10 kb) with multiple large direct repeats, rendering their syntheses technically challenging, thus hampering the use of a bottom-up approach (plug-and-play method). In such cases, a top-down approach could provide a viable alternative by allowing partial refactoring of BGCs with the minimum inputs of synthetic DNAs. As we demonstrated here, metabolome and transcriptome analyses could be used as test and learning tools, respectively, for the rational design of engineering experiments, and CRISTAR (CRISPR/Cas9-mediated TAR) provides a build-tool that allows rapid generation of the library of engineered constructs. A sequential optimization approach would effectively reduce the combinatorial complexity for engineering experiments by allowing transcriptional optimization of functionally separate operons in a stepwise-manner. The top-down synthetic biology approach we demonstrate here could be used as a general strategy for the development of high titer industrial strains of valuable secondary metabolites produced by multi-modular NRPS and type I PKS biosynthetic systems.

4. Materials and methods

4.1. Bacterial strains and culture conditions

The yeast strain *S. cerevisiae* BY4727 with the genotype of MATα his3Δ200 leu2Δ0 lys2Δ0 met15Δ0 trp1Δ63 ura3Δ0 (ATCC No. 200889) was used for all cloning and refactoring experiments. The native daptomycin producer *S. roseosporus* NRRL 11379 was acquired from the ARS culture collection (Illinois, USA). Yeast was maintained on YPD agar plates and grown overnight at 30 °C (200 rpm) prior to transformation. The LiAc/ssDNA/PEG method was used for all yeast transformation experiments (Gietz and Schiestl, 2007). Positive selection of any genetic modification was made on appropriate amino acid dropout SC (Synthetic Composite) media. *Escherichia coli* ET12567/pUZ8002 was used for all intergenic conjugations to transform plasmid DNAs into *Streptomyces*. *Streptomyces* strains were maintained on ISP4 agar and grown in R5A liquid media for lipopeptide production.

4.2. mRNA isolation

S. roseosporus NRRL 11379 was grown in rich R5A media, and RNA extraction was performed according to the previously published protocol (Bauer et al., 2017). Two milliliters of the cultures were harvested and mixed with twice the volume of RNAprotect Bacteria reagent (QIAGEN) for RNA stabilization. Mycelial cells were collected by centrifugation (4000 rpm, 10 min), and washed twice with fresh-cold water. The cell pellets were resuspended in 1 mL of Lysozyme solution (1 μg/mL in 10 mM Tris-HCl, pH 8.0) and incubated at 30 °C for 30 min. Then, the cells were disrupted by bead beating on Tissue Lyzer (QIAGEN) using 1.0 mm glass beads at 40 Hz for 5 min. The disrupted cells were collected by centrifugation (13,000 rpm, 20 min, 4 °C) and added with 1 mL of Trizol reagent for complete cell lysis. Two hundred microliters of chloroform were added to the resulting solution and centrifuged for 20 min (13,000 rpm, 4 °C). Then, 500 μL of the aqueous phases were transferred to new tubes, and nucleic acids were precipitated by adding the same volume of ice-cold ethanol. The precipitated nucleic acids were collected by centrifugation (13,000 rpm, 30 min, 4 °C), washed with 1 mL of DEPC-treated ice-cold 80% ethanol and dried at room temperature. To remove DNA, 10 μg of isolated nucleic acids were treated with 2 unit of DNAse-I (Thermo) and incubated for 30 min at 37 °C. DNA-depleted RNA samples were isolated using DNAse-free kit according to the manufacture's instruction. The resulting RNA samples were used for the preparation of sequencing libraries.

4.3. Transcriptome sequencing

The isolated RNA samples with integrity values > 7.0 and the 23s/16s rRNA ratio >1.0 were used for cDNA library construction. In briefly, 1 μg of RNA was hybridized with rRNA-specific probes, and rRNAs were immediately depleted by treating with RNase H. The rRNA-depleted samples were purified using Agencourt RNA cleanXP beads kit, and the purified RNA samples were used for the construction of sequencing libraries using a strand-specific RNA library prep kit (NEB). The constructed libraries were sequenced on the HiSeq 4000-Illumina platform with a paired-end mode, which generated more than 30 million reads with the average length of 100 bp for each replicate. Sequencing reads were processed using CLC Genomics workbench (Qiagen). Read trimming was performed to remove low quality bases (quality score: 0.05, maximum ambiguous nucleotide: 2) and adapter sequences (mismatch cost: 2, gap cost: 3, internal match minimum score: 9). Then, trimmed reads were uniquely mapped to the genome of *S. roseosporus* (GenBank Accession No.: NZ_ABYX02000001.1). The mapping results were visualized using the IGB (Integrated Genome Browser) software and used for the calculation of RPKM (Reads Per Kilobase per mapped Million) values.

4.4. Gene cluster cloning

A fosmid library (10X coverage) was constructed using the genomic DNA of *S. roseosporus* and the CopyControl Fosmid Library Production Kit (Epicentre) according to the manufacturer's instruction. The library was PCR-screened using three primer sets (Table S3) that amplify distal regions in the *dpt* cluster. Library screening was performed by whole-cell PCR using MyTaq polymerase (BioLine). Three PCR-positive clones were recovered and end-sequenced to confirm the recovery of complete *dpt* cluster. The assembly of overlapping fosmids was performed using TAR in yeast (Kim et al., 2010). The pathway-specific capture vector was constructed to contain two PCR-amplified 0.5-kb homologous sequences (UPS and DWS) flanking the *dpt* cluster. For TAR cloning, PsiI-linearized three overlapping fosmids (pSR007, pSR248, and pSR178, 1 μg of each) and HpaI-linearized capture vector (pTARb-*dpt*-CAP, 0.1 μg) were co-transformed into yeast using the LiAc/ss carrier DNA/PEG method. The resulting transformant was plated on a histidine dropout SC agar, and colonies appeared within three days. Ten colonies were picked and

inoculated into 2 mL of the same dropout SC liquid media, and plasmids were extracted from the overnight cultures using Zymolyase (ZYMO RESEARCH) lysis protocol. Miniprepped DNAs were screened by PCR with the primer set amplifying a 0.5-kb region within the *dpt* cluster (Fig. S8).

4.5. Promoter engineering

All promoter engineering experiments were performed according to our previously published mpCRISTAR protocol (Kim et al., 2020). A CRISPR plasmid targeting the promoter site was constructed using the pCRCU yeast CRISPR vector. Double stranded DNA oligomers each containing a 20 bp spacer sequence from the promoter site flanked by the BsaI recognition sequences on both ends were synthesized and cloned into pCRCU via golden gate cloning, creating site-specific CRISPR plasmids (Table S1). Next, approximately 500 bp synthetic promoter cassettes were PCR-amplified using primer sets that contain 20 bp primer sequences and 40 bp homology sequences to the flaking regions of target promoter sites (Table S3). For promoter engineering, yeast was first transformed with site-specific CRISPR plasmids, and selected on the appropriate drop-out SC agar plates. Then, promoter cassettes (2 μg of each) and the *dpt* cluster (2 μg) were co-transformed into yeast already expressing Cas9 and gRNAs, and the transformants were selected on appropriate amino acids drop-out SC agar plates. Ten colonies were picked from each plate and inoculated into 2 mL of the same drop-out SC liquid media. DNA mini-prep was performed using the overnight cultures according to a Zymolyase lysis protocol. The correct insertions of promoter cassettes into desired promoter sites were confirmed by PCR-based genotyping using the primer sets (Table S2) that generate amplicons bridging between the *dpt* cluster and newly inserted promoter cassettes.

4.6. CRISPR/Cas9-based genome editing

The deletion of a large genomic region (*dpt* cluster or *bkd* operon) in *S. roseosporus* was performed using pCRISPomyces-2 (Cobb et al., 2015). Briefly, the 1 kb homologous sequences flanking a deletion region were PCR-amplified using primer sets containing 20 bp primer sequences and 40 bp homology sequences to pCRISPomyces-2 (Table S1). Then, the purified PCR products (1 μg of each) and HpaI-linearized pCRISPomyces-2 were co-transformed into yeast for TAR cloning, creating the homology arm-containing CRISPR plasmid (pCRISPomyces-*dptHR* or pCRISPomyces-*bkdHR*). A double-stranded DNA fragment containing the sequence of *spacer1-scaffold-terminator-GAPDHp-spacer2* flanked by 20 bp sequences homologous to pCRISPomyces-2 was synthesized and cloned into pCRISPomyces-*HR* via Gibson assembly (NEB), creating the deletion target-specific CRISPR plasmid (pCRISPomyces-*dptKO* or pCRISPomyces-*bkdKO*). The successful cloning of both homology arms and gRNA spacer sequences were confirmed by Sanger-sequencing. The resulting target-specific CRISPR plasmid was transferred into *S. roseosporus* via intergenic conjugation. Ten *Streptomyces* colonies were re-patched on ISP4 agar plates containing apramycin and nalidixic acids and were grown in TSB liquid media for 3 days for DNA isolation. Successful deletion was confirmed by PCR-based genotyping using primer sets designed from the outside of a deletion region, and PCR amplicons with a correct size were sanger-sequenced. After confirming the successful deletion, the CRISPR plasmid was cleared from the cells by growing in TSB liquid media at 37 °C for 4 days, and the plasmid clearance was confirmed by testing apramycin sensitivity.

4.7. Lipopeptide production

Refactored *dpt** gene clusters were transformed into *E. coli* ET12567/pUZ8002 strain and then transferred into *Streptomyces* via intergenic conjugation. For lipopeptide production, spores were inoculated into R5A rich media and grown at 30 °C with shaking (200 rpm). After 7 days, 50 μL of the culture broth was collected and filtered through 0.45 μm membrane. The resulting samples were analyzed on reversed-phase HPLC using a C_{18} analytical column (4.6 × 150 mm, 5 μm) and solvent gradient from 5% to 100% acetonitrile in water containing 0.1% trifluoroacetic acid with the flow rate of 1 mL/min. The lipopeptide titer was calculated by measuring the area under a peak at 222 nm. The calibration curve was created using pure daptomycin (TCI) dissolved in water at various concentrations (Fig. S19). For decanoic acid feeding experiments, *Streptomyces* spores were inoculated into 2 mL of TSB liquid media and grown for 3 days at 30° with shaking (200 rpm). The 1 mL of saturated seed culture was inoculated into 50 mL of R5A liquid media in 250 mL baffled flask and grown for 48 h. Then, decanoic acid was supplied into the culture media every 12 h at the final concentration of 0.5 mM for 7 days. The titers of daptomycin and related-lipopeptides were calculated in the same way as described above.

Author statements

Chang-Hun Ji and Hahk-Soo Kang designed experiments. Chang-Hun Ji conducted all experiments. Hiyoung Kim and Dongho Lee helped with the isolation and structure determination of compounds **5** and **6**. Haeun Kwon performed the LC-MS analysis of compounds **5** and **6**. Hyun-Woo Je helped with the Streptomyces genome editing. Chang-Hun Ji and Hahk-Soo Kang wrote the manuscript.

Declaration of competing interest

The authors declare no conflicts of interest.

Acknowledgements

This work was supported by the Grants from the National Research Foundation of Korea (NRF-2018R1C1B3001028, and NRF-2019R1A4A1020626). C.-H.J. received the financial support from the NRF-Korea through Global Ph.D. Fellowship program (NRF-2019H1A2A1073592).

Appendix A. Supplementary data

Supplementary data to this article can be found online at https://doi.org/10.1016/j.ymben.2021.10.013.

References

Ajikumar, P.K., Xiao, W.H., Tyo, K.E., Wang, Y., Simeon, F., Leonard, E., Mucha, O., Phon, T.H., Pfeifer, B., Stephanopoulos, G., 2010. Isoprenoid pathway optimization for Taxol precursor overproduction in Escherichia coli. Science 330, 70–74.

Alper, H.S., Avalos, J.L., 2018. Metabolic pathway engineering. Synth Syst Biotechnol 3, 1–2.

Amos, G.C.A., Awakawa, T., Tuttle, R.N., Letzel, A.C., Kim, M.C., Kudo, Y., Fenical, W., Moore, B.S., Jensen, P.R., 2017. Comparative transcriptomics as a guide to natural product discovery and biosynthetic gene cluster functionality. Proc. Natl. Acad. Sci. U. S. A. 114, E11121–E11130.

Atanasov, A.G., Zotchev, S.B., Dirsch, V.M., International Natural Product Sciences, T., Supuran, C.T., 2021. Natural products in drug discovery: advances and opportunities. Nat. Rev. Drug Discov. 20, 200–216.

Baltz, R.H., 2021. Genome mining for drug discovery: cyclic lipopeptides related to daptomycin. J. Ind. Microbiol. Biotechnol. 48.

Bauer, J.S., Fillinger, S., Forstner, K., Herbig, A., Jones, A.C., Flinspach, K., Sharma, C., Gross, H., Nieselt, K., Apel, A.K., 2017. dRNA-seq transcriptional profiling of the FK506 biosynthetic gene cluster in Streptomyces tsukubaensis NRRL18488 and general analysis of the transcriptome. RNA Biol. 14, 1617–1626.

Behsaz, B., Bode, E., Gurevich, A., Shi, Y.N., Grundmann, F., Acharya, D., Caraballo-Rodriguez, A.M., Bouslimani, A., Panitchpakdi, M., Linck, A., Guan, C., Oh, J., Dorrestein, P.C., Bode, H.B., Pevzner, P.A., Mohimani, H., 2021. Integrating genomics and metabolomics for scalable non-ribosomal peptide discovery. Nat. Commun. 12, 3225.

Blin, K., Shaw, S., Steinke, K., Villebro, R., Ziemert, N., Lee, S.Y., Medema, M.H., Weber, T., 2019. antiSMASH 5.0: updates to the secondary metabolite genome mining pipeline. Nucleic Acids Res. 47, W81–W87.

Chen, X., Wei, P., Fan, L., Yang, D., Zhu, X., Shen, W., Xu, Z., Cen, P., 2009. Generation of high-yield rapamycin-producing strains through protoplasts-related techniques. Appl. Microbiol. Biotechnol. 83, 507–512.
Cobb, R.E., Wang, Y., Zhao, H., 2015. High-efficiency multiplex genome editing of Streptomyces species using an engineered CRISPR/Cas system. ACS Synth. Biol. 4, 723–728.
Dahabieh, M.S., Thevelein, J.M., Gibson, B., 2020. Multimodal microorganism development: integrating top-down biological engineering with bottom-up rational design. Trends Biotechnol. 38, 241–253.
Debono, M., Barnhart, M., Carrell, C.B., Hoffmann, J.A., Occolowitz, J.L., Abbott, B.J., Fukuda, D.S., Hamill, R.L., Biemann, K., Herlihy, W.C., 1987. A21978C, a complex of new acidic peptide antibiotics: isolation, chemistry, and mass spectral structure elucidation. J. Antibiot. (Tokyo) 40, 761–777.
Demain, A.L., 2014. Importance of microbial natural products and the need to revitalize their discovery. J. Ind. Microbiol. Biotechnol. 41, 185–201.
Gal, M.C., Thurston, L., Rich, P., Miao, V., Baltz, R.H., 2006. Complementation of daptomycin dptA and dptD deletion mutations in trans and production of hybrid lipopeptide antibiotics. Microbiology (Read.) 152, 2993–3001.
Gao, H., Liu, M., Zhou, X., Liu, J., Zhuo, Y., Gou, Z., Xu, B., Zhang, W., Liu, X., Luo, A., Zheng, C., Chen, X., Zhang, L., 2010. Identification of avermectin-high-producing strains by high-throughput screening methods. Appl. Microbiol. Biotechnol. 85, 1219–1225.
Gao, Y., Zhao, Y., He, X., Deng, Z., Jiang, M., 2021. Challenges of functional expression of complex polyketide biosynthetic gene clusters. Curr. Opin. Biotechnol. 69, 103–111.
Gietz, R.D., Schiestl, R.H., 2007. High-efficiency yeast transformation using the LiAc/SS carrier DNA/PEG method. Nat. Protoc. 2, 31–34.
Gonzalez-Ruiz, A., Seaton, R.A., Hamed, K., 2016. Daptomycin: an evidence-based review of its role in the treatment of Gram-positive infections. Infect. Drug Resist. 9, 47–58.
Gotze, S., Arp, J., Lackner, G., Zhang, S., Kries, H., Klapper, M., Garcia-Altares, M., Willing, K., Gunther, M., Stallforth, P., 2019. Structure elucidation of the syringafactin lipopeptides provides insight in the evolution of nonribosomal peptide synthetases. Chem. Sci. 10, 10979–10990.
Grunewald, J., Sieber, S.A., Mahlert, C., Linne, U., Marahiel, M.A., 2004. Synthesis and derivatization of daptomycin: a chemoenzymatic route to acidic lipopeptide antibiotics. J. Am. Chem. Soc. 126, 17025–17031.
Huang, X., Ma, T., Tian, J., Shen, L., Zuo, H., Hu, C., Liao, G., 2017. wblA, a pleiotropic regulatory gene modulating morphogenesis and daptomycin production in Streptomyces roseosporus. J. Appl. Microbiol. 123, 669–677.
Huber, F.M., Pieper, R.L., Tietz, A.J., 1988. The formation of daptomycin by supplying decanoic acid to streptomyces-roseosporus cultures producing the antibiotic complex A21978c. J. Biotechnol. 7, 283–292.
Ji, C.H., Kim, J.P., Kang, H.S., 2018. Library of synthetic Streptomyces regulatory sequences for use in promoter engineering of natural product biosynthetic gene clusters. ACS Synth. Biol. 7, 1946–1955.
Kim, H., Ji, C.H., Je, H.W., Kim, J.P., Kang, H.S., 2020. mpCRISTAR: multiple plasmid approach for CRISPR/Cas9 and TAR-mediated multiplexed refactoring of natural product biosynthetic gene clusters. ACS Synth. Biol. 9, 175–180.
Kim, J.H., Feng, Z., Bauer, J.D., Kallifidas, D., Calle, P.Y., Brady, S.F., 2010. Cloning large natural product gene clusters from the environment: piecing environmental DNA gene clusters back together with TAR. Biopolymers 93, 833–844.
Lee, S.K., Kim, H.R., Jin, Y.Y., Yang, S.H., Suh, J.W., 2016. Improvement of daptomycin production via increased resistance to decanoic acid in Streptomyces roseosporus. J. Biosci. Bioeng. 122, 427–433.
Lee, Y., Lee, N., Hwang, S., Kim, K., Kim, W., Kim, J., Cho, S., Palsson, B.O., Cho, B.K., 2020. System-level understanding of gene expression and regulation for engineering secondary metabolite production in Streptomyces. J. Ind. Microbiol. Biotechnol. 47, 739–752.
Liao, G., Liu, Q., Xie, J., 2013a. Transcriptional analysis of the effect of exogenous decanoic acid stress on Streptomyces roseosporus. Microb. Cell Factories 12, 19.
Liao, G., Wang, L., Liu, Q., Guan, F., Huang, Y., Hu, C., 2013b. Manipulation of kynurenine pathway for enhanced daptomycin production in Streptomyces roseosporus. Biotechnol. Prog. 29, 847–852.
Lim, H.N., Lee, Y., Hussein, R., 2011. Fundamental relationship between operon organization and gene expression. Proc. Natl. Acad. Sci. U. S. A. 108, 10626–10631.
Lu, W., Fan, J., Wen, J., Xia, Z., Caiyin, Q., 2011. Kinetic analysis and modeling of daptomycin batch fermentation by Streptomyces roseosporus. Appl. Biochem. Biotechnol. 163, 453–462.
Luo, S., Chen, X.A., Mao, X.M., Li, Y.Q., 2018. Transposon-based identification of a negative regulator for the antibiotic hyper-production in Streptomyces. Appl. Microbiol. Biotechnol. 102, 6581–6592.
Mao, X.M., Luo, S., Li, Y.Q., 2017. Negative regulation of daptomycin production by DepR2, an ArsR-family transcriptional factor. J. Ind. Microbiol. Biotechnol. 44, 1653–1658.
Mao, X.M., Luo, S., Zhou, R.C., Wang, F., Yu, P., Sun, N., Chen, X.X., Tang, Y., Li, Y.Q., 2015. Transcriptional regulation of the daptomycin gene cluster in Streptomyces roseosporus by an autoregulator, AtrA. J. Biol. Chem. 290, 7992–8001.
Miao, V., Coeffet-LeGal, M.F., Brian, P., Brost, R., Penn, J., Whiting, A., Martin, S., Ford, R., Parr, I., Bouchard, M., Silva, C.J., Wrigley, S.K., Baltz, R.H., 2005. Daptomycin biosynthesis in Streptomyces roseosporus: cloning and analysis of the gene cluster and revision of peptide stereochemistry. Microbiology (Read.) 151, 1507–1523.
Montiel, D., Kang, H.S., Chang, F.Y., Charlop-Powers, Z., Brady, S.F., 2015. Yeast homologous recombination-based promoter engineering for the activation of silent natural product biosynthetic gene clusters. Proc. Natl. Acad. Sci. U. S. A. 112, 8953–8958.
Ng, I.S., Ye, C., Zhang, Z., Lu, Y., Jing, K., 2014. Daptomycin antibiotic production processes in fed-batch fermentation by Streptomyces roseosporus NRRL11379 with precursor effect and medium optimization. Bioproc. Biosyst. Eng. 37, 415–423.
Nguyen, K.T., Kau, D., Gu, J.Q., Brian, P., Wrigley, S.K., Baltz, R.H., Miao, V., 2006. A glutamic acid 3-methyltransferase encoded by an accessory gene locus important for daptomycin biosynthesis in Streptomyces roseosporus. Mol. Microbiol. 61, 1294–1307.
Palazzotto, E., Tong, Y., Lee, S.Y., Weber, T., 2019. Synthetic biology and metabolic engineering of actinomycetes for natural product discovery. Biotechnol. Adv. 37, 107366.
Patridge, E., Gareiss, P., Kinch, M.S., Hoyer, D., 2016. An analysis of FDA-approved drugs: natural products and their derivatives. Drug Discov. Today 21, 204–207.
Sharan, S.K., Thomason, L.C., Kuznetsov, S.G., Court, D.L., 2009. Recombineering: a homologous recombination-based method of genetic engineering. Nat. Protoc. 4, 206–223.
Sharma, C.M., Hoffmann, S., Darfeuille, F., Reignier, J., Findeiss, S., Sittka, A., Chabas, S., Reiche, K., Hackermuller, J., Reinhardt, R., Stadler, P.F., Vogel, J., 2010. The primary transcriptome of the major human pathogen Helicobacter pylori. Nature 464, 250–255.
Smanski, M.J., Bhatia, S., Zhao, D., Park, Y., Woodruff, L.B.A., Giannoukos, G., Ciulla, D., Busby, M., Calderon, J., Nicol, R., Gordon, D.B., Densmore, D., Voigt, C.A., 2014. Functional optimization of gene clusters by combinatorial design and assembly. Nat. Biotechnol. 32, 1241–1249.
Smanski, M.J., Zhou, H., Claesen, J., Shen, B., Fischbach, M.A., Voigt, C.A., 2016. Synthetic biology to access and expand nature's chemical diversity. Nat. Rev. Microbiol. 14, 135–149.
Song, C., Luan, J., Cui, Q., Duan, Q., Li, Z., Gao, Y., Li, R., Li, A., Shen, Y., Li, Y., Stewart, A.F., Zhang, Y., Fu, J., Wang, H., 2019. Enhanced heterologous spinosad production from a 79-kb synthetic multioperon assembly. ACS Synth. Biol. 8, 137–147.
Song, C., Luan, J., Li, R., Jiang, C., Hou, Y., Cui, Q., Cui, T., Tan, L., Ma, Z., Tang, Y.J., Stewart, A.F., Fu, J., Zhang, Y., Wang, H., 2020. RedEx: a method for seamless DNA insertion and deletion in large multimodular polyketide synthase gene clusters. Nucleic Acids Res. 48, e130.
Tian, T., Salis, H.M., 2015. A predictive biophysical model of translational coupling to coordinate and control protein expression in bacterial operons. Nucleic Acids Res. 43, 7137–7151.
Wang, F., Ren, N.N., Luo, S., Chen, X.X., Mao, X.M., Li, Y.Q., 2014. DptR2, a DeoR-type auto-regulator, is required for daptomycin production in Streptomyces roseosporus. Gene 544, 208–215.
Westfall, P.J., Pitera, D.J., Lenihan, J.R., Eng, D., Woolard, F.X., Regentin, R., Horning, T., Tsuruta, H., Melis, D.J., Owens, A., Fickes, S., Diola, D., Benjamin, K.R., Keasling, J.D., Leavell, M.D., McPhee, D.J., Renninger, N.S., Newman, J.D., Paddon, C.J., 2012. Production of amorphadiene in yeast, and its conversion to dihydroartemisinic acid, precursor to the antimalarial agent artemisinin. Proc. Natl. Acad. Sci. U. S. A. 109, E111–E118.
Wittmann, M., Linne, U., Pohlmann, V., Marahiel, M.A., 2008. Role of DptE and DptF in the lipidation reaction of daptomycin. FEBS J. 275, 5343–5354.
Yamanaka, K., Reynolds, K.A., Kersten, R.D., Ryan, K.S., Gonzalez, D.J., Nizet, V., Dorrestein, P.C., Moore, B.S., 2014. Direct cloning and refactoring of a silent lipopeptide biosynthetic gene cluster yields the antibiotic taromycin A. Proc. Natl. Acad. Sci. U. S. A. 111, 1957–1962.
Ye, C., Ng, I.S., Jing, K., Lu, Y., 2014. Direct proteomic mapping of Streptomyces roseosporus NRRL 11379 with precursor and insights into daptomycin biosynthesis. J. Biosci. Bioeng. 117, 591–597.
Yu, G., Hu, Y., Hui, M., Chen, L., Wang, L., Liu, N., Yin, Y., Zhao, J., 2014. Genome shuffling of Streptomyces roseosporus for improving daptomycin production. Appl. Biochem. Biotechnol. 172, 2661–2669.
Yu, G., Hui, M., Li, R., Zhang, S., 2020. Pleiotropic regulation of daptomycin synthesis by DptR1, a LuxR family transcriptional regulator. World J. Microbiol. Biotechnol. 36, 173.
Yu, G., Jia, X., Wen, J., Lu, W., Wang, G., Caiyin, Q., Chen, Y., 2011. Strain improvement of Streptomyces roseosporus for daptomycin production by rational screening of He-Ne laser and NTG induced mutants and kinetic modeling. Appl. Biochem. Biotechnol. 163, 729–743.
Zhang, D., Wang, X., Ye, Y., He, Y., He, F., Tian, Y., Luo, Y., Liang, S., 2021. Label-free proteomic dissection on dptP-deletion mutant uncovers dptP involvement in strain growth and daptomycin tolerance of Streptomyces roseosporus. Microb Biotechnol 14, 708–725.
Zummo, F.P., Marineo, S., Pace, A., Civiletti, F., Giardina, A., Puglia, A.M., 2012. Tryptophan catabolism via kynurenine production in Streptomyces coelicolor: identification of three genes coding for the enzymes of tryptophan to anthranilate pathway. Appl. Microbiol. Biotechnol. 94, 719–728.
Zuttion, F., Colom, A., Matile, S., Farago, D., Pompeo, F., Kokavecz, J., Galinier, A., Sturgis, J., Casuso, I., 2020. High-speed atomic force microscopy highlights new molecular mechanism of daptomycin action. Nat. Commun. 11, 6312.